SNS 110040300-TR0002-R00

Poison Depth Sensitivity Studies for the SNS Parahydrogen Moderator

March 2003

A U.S. Department of Energy Multilaboratory Project
SPALLATION NEUTRON SOURCE
Argonne National Laboratory • Brookhaven National Laboratory • Thomas Jefferson National Accelerator Facility • Lawrence Berkeley National Laboratory • Los Alamos National Laboratory • Oak Ridge National Laboratory
SNS

Poison Depth Sensitivity Studies for the SNS Parahydrogen Moderator
SNS 110040300-TR0002-R00

E. B. Iverson P. D. Ferguson

Date Published: March 2003

Prepared for the
U.S. Department of Energy
Office of Science

UT-BATTELLE, LLC
managing
Spallation Neutron Source activities at

Argonne National Laboratory
Brookhaven National Laboratory
Thomas Jefferson National Accelerator Facility
Lawrence Berkeley National Laboratory
Los Alamos National Laboratory
Oak Ridge National Laboratory

under contract DE-AC05-00OR22725
for the
U.S. DEPARTMENT OF ENERGY

This document describes the variation in decoupled poisoned hydrogen moderator performance when using different gadolinium poison depths. The sensitivity calculations are performed relative to the SCT base case described more fully elsewhere.[1]

1 Model Description

The base configuration we denote SCT includes four moderators, two of which are viewed from both sides. All moderators have nominal viewed faces of 100 mm (horizontal) by 120 mm (vertical). The inner reflector (out to a radius of ≈320 mm) is beryllium and is cooled with heavy water. This inner reflector is surrounded by heavy water-cooled stainless steel. Table 1 summarizes relevant characteristics of the target station configuration used for this set of calculations. Although the SNS is designed for 2 MW operation as shown in Table 1, the initial construction will provide 1.44 MW operation. As our past calculations are normalized for 2 MW operation, we present these calculations with that same normalization.

Proton Energy	1 GeV
Pulse Rate	60 Hz
Average Power	2 MW
Energy per pulse	34 kJ
Proton Beam Shape	rectangular
Proton Beam Size	200x70 mm^2
Proton Pulse	$\delta(t)$
Target	Hg
Inner Reflector	Be
I.R. Coolant	D_2O
Outer Reflector	SS
O.R. Coolant	D_2O

Table 1: Target station parameters used in calculations. All normalizations are performed per 34 kJ-pulse.

Figure 1 illustrates and Table 2 summarizes the moderator configuration. The top upstream moderator, the one varied for this study, is cadmium-decoupled hydrogen (assumed to be 100% parahydrogen) at 20 K and has curved viewed surfaces. The moderator material has a maximum thickness of 60 mm, and an average thickness of about 55 mm. The moderator is (in the base case) poisoned at the centerline with gadolinium 0.8 mm thick and is viewed

Beamline	Moderator Location	Moderator Material	T (K)	Decoupling Material	Poison Material	Poison Depth (mm)
2	TU	H_2	20	Cd	Gd	29.6
11	TU	H_2	20	Cd	Gd	29.6
5	TD	H_2	20	–	–	–
14	BD	H_2	20	–	–	–
8	BU	H_2O	300	Cd	Gd	14.75
17	BU	H_2O	300	Cd	Gd	24.75

Table 2: Moderator summary. H_2 is 20 K supercritical, modeled as liquid parahydrogen at supercritical density.

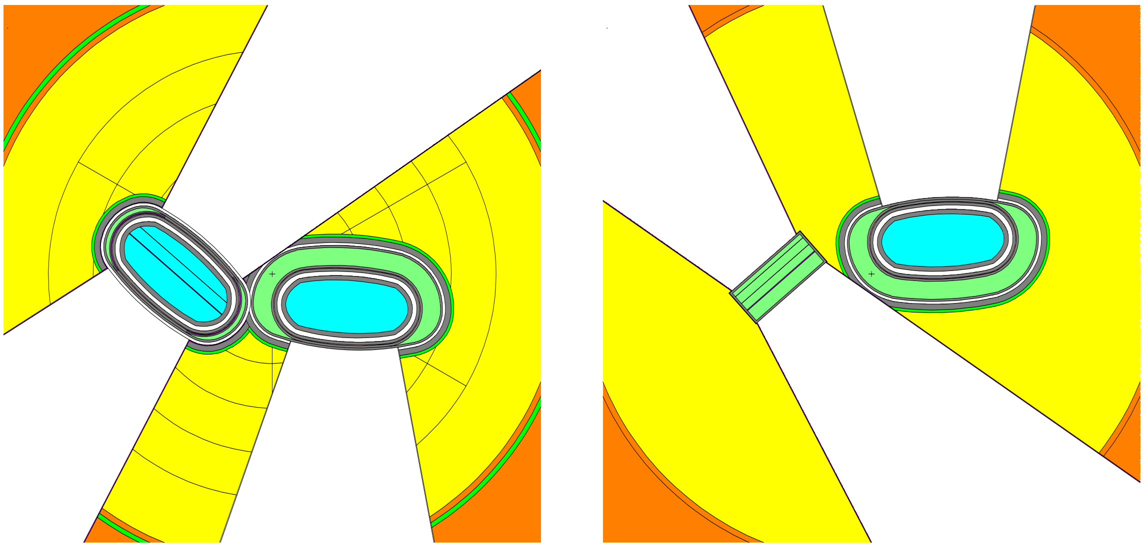

(a) Top Moderators (b) Bottom Moderators

Figure 1: SNS moderator configuration. Elevations shown are the centers of the upstream moderators. Protons enter from the left. Beamlines are numbered counterclockwise beginning at the proton beam.

from both sides. The top downstream moderator is fully coupled unpoisoned hydrogen (again parahydrogen) at 20 K, and is viewed from one side only. This moderator also has a curved viewed surface, with maximum thickness of 60 mm, and an average thickness of about 55 mm. This moderator also has approximately 20 mm of light water surrounding it as premoderator. The bottom downstream moderator is identical to the top downstream moderator. The bottom upstream moderator is cadmium-decoupled water at 300 K with flat viewed surfaces. The moderator material is 40.5 mm thick, and is assymetrically poisoned with gadolinium 1 mm thick. This moderator is viewed from both sides. These poison depth sensitivity calculations concern only the top upstream moderator.

2 Calculational Techniques

The simulations reported are the results of calculations using the MCNPX code from LANL (version 2.1.5).[2] The spectral intensities shown result from calculations using point detector tallies located 10 m from the viewed surface of the moderator. Artificial collimating masks between the point detector locations and the moderator surfaces limit the tallied view of the moderator to a 100 mm horizontal by 120 mm vertical view of the moderator, centered on the viewed face. The emission time distributions (pulse shapes) come from current tallies on the viewed surface of the moderator material, and are averaged over 2π steradians. Weight windows to accelerate the pulse shape calculations were generated by separate iterative runs using MCNPX in parallel mode on a large cluster of machines with a neutron-only source term. MCNPX runs using these weight windows produced the reported results, which have further been scaled (from the point detector calculations) to correspond to the peak intensity coming off of the moderator face in the normal direction, rather than the average over 2π steradians. In this set of sensitivity calculations, we generated a single set of weight windows and used them for each of the different poison depth calculations on the decoupled hydrogen moderator. In these calculations, we use our standard set of parahydrogen scattering kernels, the kernel made available by LANL to the ACoM collaboration after the International Workshop on Cold Moderators at Pulsed Neutron Sources.[3]

3 Observations

Exhaustive plots of spectra, emission time distributions, and various pulse shape metrics appears in Appendix B. We repeat some of that data here as illustration to our observations. The beam intensity and a metric (full-width at half-maximum) for the width of the energy-dependent pulse shape as calculated for a decoupled poisoned hydrogen moderator appear in Figure 2. Note that the nominal SCT poison depth is 29.6 mm.

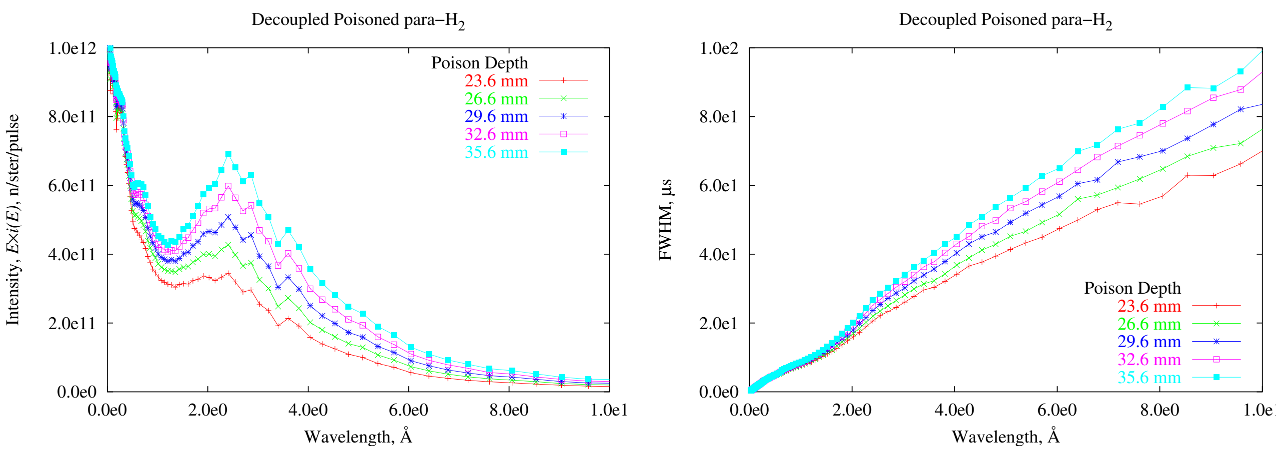

Figure 2: Intensity and pulse widths (FWHM) for decoupled poisoned parahydrogen moderators with different poison depths. The nominal poison depth for the SCT base case is 29.6 mm.

We clearly see significant differences between the moderator performance predictions for different poison depths. The differences are relatively straightforward and predictable, with deeper poisoning giving greater integrated intensity, greater pulse width, and greater peak intensity. As an example, for 5.62 meV neutrons, the integrated intensity variation over the poison depth range reported runs from a 35% loss to a 40% gain, the pulse width (FWHM) variation from a 15% decrease to a 15% increase, and the peak intensity variation from a 25% loss to a 25% gain (see Figure 3). Selection of the appropriate poison depth will require more detailed instrument-based optimization studies. It is also worth noting that, for these 100% parahydrogen moderators, the poison depth does not change the long-time asymptotic decay of the pulse shape distribution (often referred to as the “tails”) for a given energy (see Figure 4(a)). This is a demonstration of the non-thermalizing nature of the parahydrogen moderator. Further demonstration of this non-thermalizing nature comes from an examination of the pulse shapes for different energies at a given poison depth, as shown in Figure 4(b), where the decay of the pulse shape never approaches a consistent value independent of energy as is the case for thermalizing moderators. One final indication is the behavior of the RMS deviation of the pulse width, as shown in Figure 5, where there is little difference as a function of poison depth. One might conclude, at least on the basis of this study, that the pulse shape RMS deviation is not a particularly sensitive metric for pulse width for a decoupled parahydrogen moderator.

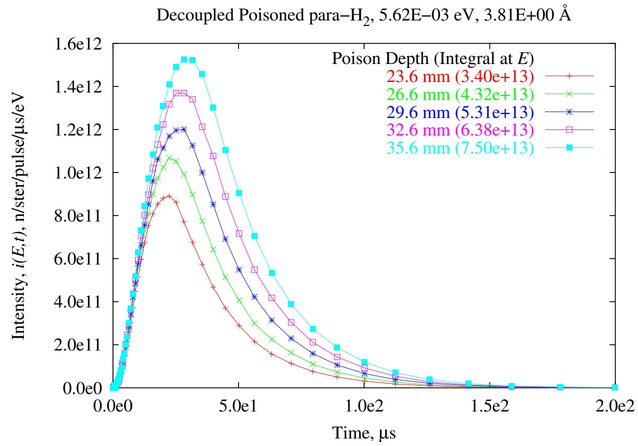

Figure 3: Emission time distributions for 5.62 meV neutrons from decoupled poisoned parahydrogen moderators with different poison depths.

4 Parameterization

As described elsewhere[1] we use the function

$$i(E) = I_{\rm epi} e^{-c/\sqrt{E}} \left(R \frac{E}{(kT)^2} e^{-E/kT} + \Delta(E)\rho(E)\frac{1}{E^{1-\alpha}} \right), \tag{1}$$

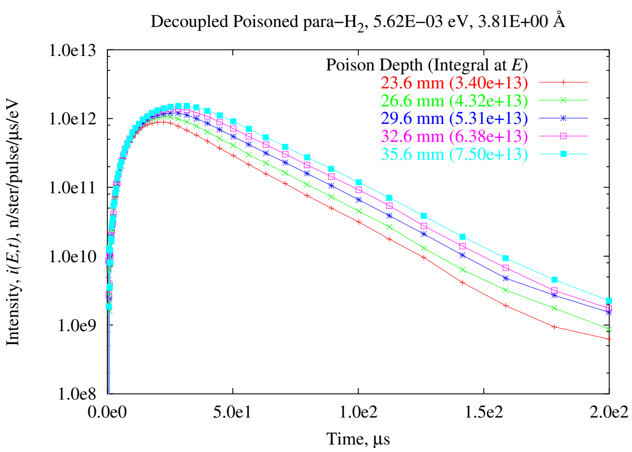

(a) Multiple poison depths at a single energy.

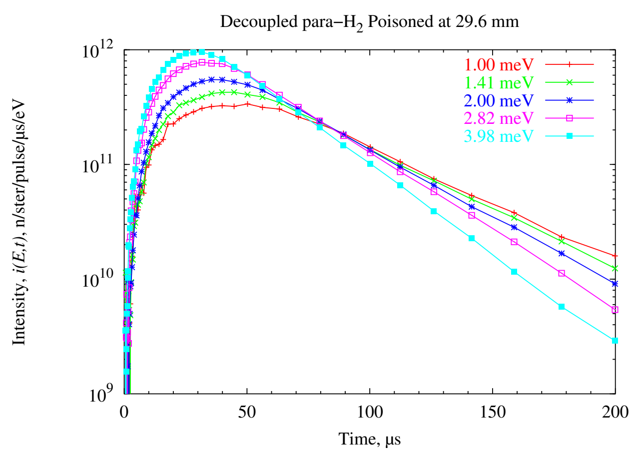

(b) Multiple energies at a single poison depth.

Figure 4: Emission time distributions showing the non-thermalizing nature of parahydrogen moderators.

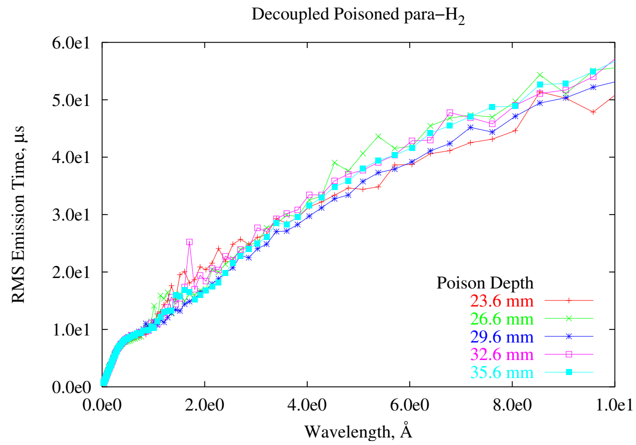

Figure 5: RMS emission times for different poison depths.

with a generalized Westcott joining function,

$$\Delta(E) = \frac{1}{1 + (E_{\mathrm{co}}/E)^s} \tag{2}$$

to couple a slowing-down term to a Maxwellian, with a function

$$\rho(E) = 1 + \delta_\rho e^{-x}\left(1 + x + \frac{1}{2}x^2\right), \tag{3}$$

where

$$x(E) = \begin{cases} \gamma(E - 2B) & E > 2B \\ 0 & E \leq 2B, \end{cases} \tag{4}$$

"chosen to simulate the rapid change in the para-hydrogen cross section at $2B$," to fit the spectra from the hydrogen moderators, as shown in Figure 6. B is the free hydrogen rotational constant (7.36 meV), and δ_ρ and γ are fitted parameters.[4]

Parameters resulting from such fits are shown in Table 3. Although these parameterizations are inspired by a physics analysis of neutron slowing-down and thermalization, they do not model the simulated data well enough to have unique physical interpretations, and should be considered arbitrary "smoothing" functions. Although the general agreement appears good, χ^2_ν is high, typically around 400-2100. Although the quality of the fits shown in Figure 6 is only moderate, the fits can certainly be trusted to predict absolute performance to better than 10% over the energy range 0.001–10 eV, and to predict relative trends to somewhat better precision.

References

[1] E. B. Iverson, P. D. Ferguson, F. X. Gallmeier, and I. I. Popova, "Detailed SNS neutronics calculations for scattering instrument design: SCT configuration," Tech. Rep. SNS 110040300-DA0001-R00, Oak Ridge National Laboratory, July 2002.

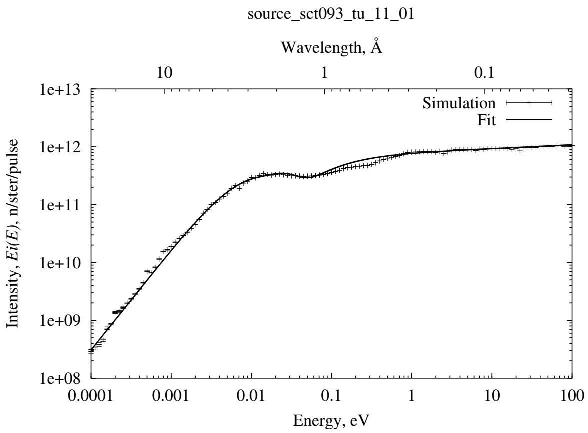

(a) Poison Depth of 23.6 mm.

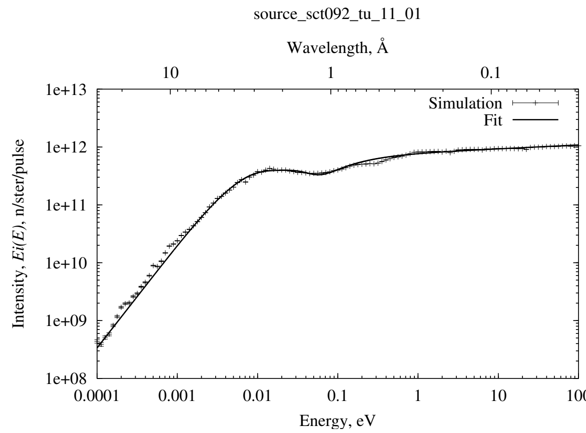

(b) Poison Depth of 26.6 mm.

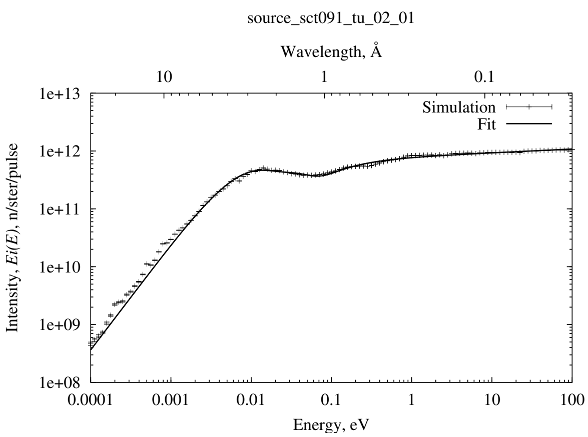

(c) Poison Depth of 29.6 mm.

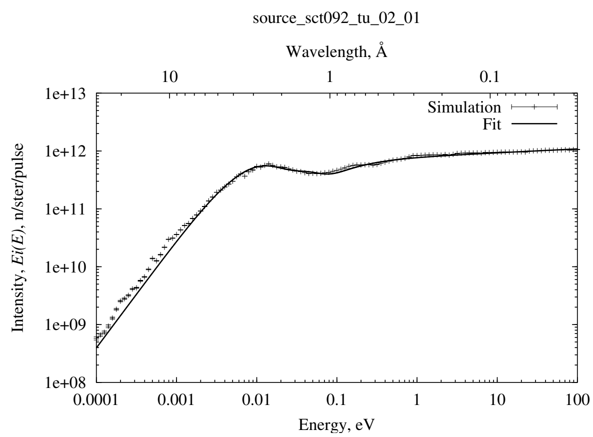

(d) Poison Depth of 32.6 mm.

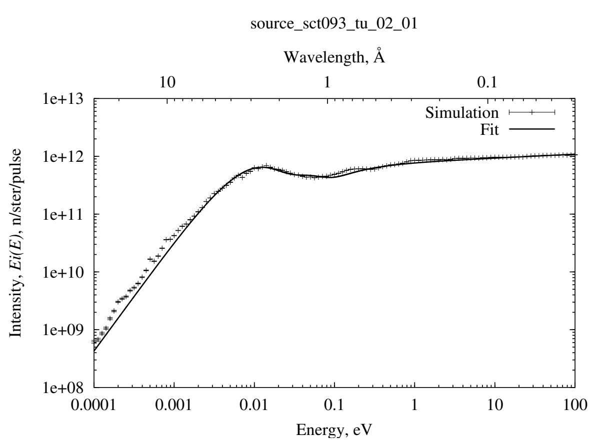

(e) Poison Depth of 35.6 mm.

Figure 6: Parametric fits to the spectral intensities from parahydrogen moderators of different poison depths.

Poison Depth	Moderator	I_{epi} n/ster/eV/pulse	kT meV	R -	c $\sqrt{\mathrm{eV}}$	E_{co} meV	s -	α -	δ_ρ -	γ eV^{-1}
23.6	dec. pois. H_2	8.0×10^{11}	4.5	0.37	0.005	72.	1.23	0.066	1.75	155.
26.6	dec. pois. H_2	8.0×10^{11}	4.8	0.57	0.005	72.	1.23	0.066	1.75	124.
29.6	dec. pois. H_2	8.0×10^{11}	5.0	0.77	0.005	72.	1.23	0.066	1.70	103.
32.6	dec. pois. H_2	8.0×10^{11}	5.1	0.99	0.005	72.	1.23	0.067	1.67	87.
35.6	dec. pois. H_2	8.0×10^{11}	5.2	1.22	0.005	72.	1.23	0.067	1.65	76.

Table 3: Spectral parameterizations of parahydrogen moderator spectral intensities.

[2] L. S. Waters, "MCNPX$^{\mathrm{tm}}$ user's manual," Tech. Rep. LA-UR 99-6058, Los Alamos National Laboratory, November 1999.

[3] R. E. MacFarlane, "Cold-moderator scattering kernel methods," in *Proceedings of the International Workshop on Cold Moderators for Pulsed Neutron Sources* (J. M. Carpenter and E. B. Iverson, eds.), pp. 221–231, OECD, 1998.

[4] T. O. Brun, "Spectra and pulse shapes of a decoupled liquid hydrogen moderator," in *Proceedings of the International Workshop on Cold Moderators for Pulsed Neutron Sources* (J. M. Carpenter and E. B. Iverson, eds.), pp. 163–170, OECD, 1998.

A Data Availability

These results are available electronically as "source files;" ASCII files containing the spectra and emission time distributions, with comments showing the file format. Each moderator–poison depth combination is represented by a single source file. These source files can be downloaded from http://www.sns.anl.gov under "Components/Moderators." Various "metrics" characterizing the spectra and pulse shapes are sometimes more useful than the fully detailed source. We have calculated the following metrics for each neutron beam:

- total intensity,
- peak intensity,
- peak time,
- full-width at half-maximum,
- mean emission time, and
- root-mean-square emission time.

These metrics are also available at the same location. Datasets are associated with source files and metrics files as given in Table 4. Note that, as the file names indicate, the calculations for the shallower poison depths were performed for the beamline 11 side of the moderator, while the remaining poison depths concern the beamline 2 side of the moderator; this permitted parallel calculation of different quantities, and does not impact the comparison on the basis of poison depth.

Poison Depth (mm)	Moderator	Source File	Metrics File
23.6	dec. pois. H_2	`source_sct093_tu_11_1.dat`	`source_sct093_tu_11_1_metrics.dat`
26.6	dec. pois. H_2	`source_sct092_tu_11_1.dat`	`source_sct092_tu_11_1_metrics.dat`
29.6	dec. pois. H_2	`source_sct091_tu_02_1.dat`	`source_sct091_tu_02_1_metrics.dat`
32.6	dec. pois. H_2	`source_sct092_tu_02_1.dat`	`source_sct092_tu_02_1_metrics.dat`
35.6	dec. pois. H_2	`source_sct093_tu_02_1.dat`	`source_sct093_tu_02_1_metrics.dat`

Table 4: Source file and metrics file names.

B Detailed Spectra and Pulse Shapes

Some of the detailed spectra and pulse shapes as produced with the simulations appear below. These plots represent only a fraction of the information available from the detailed source and metrics files.

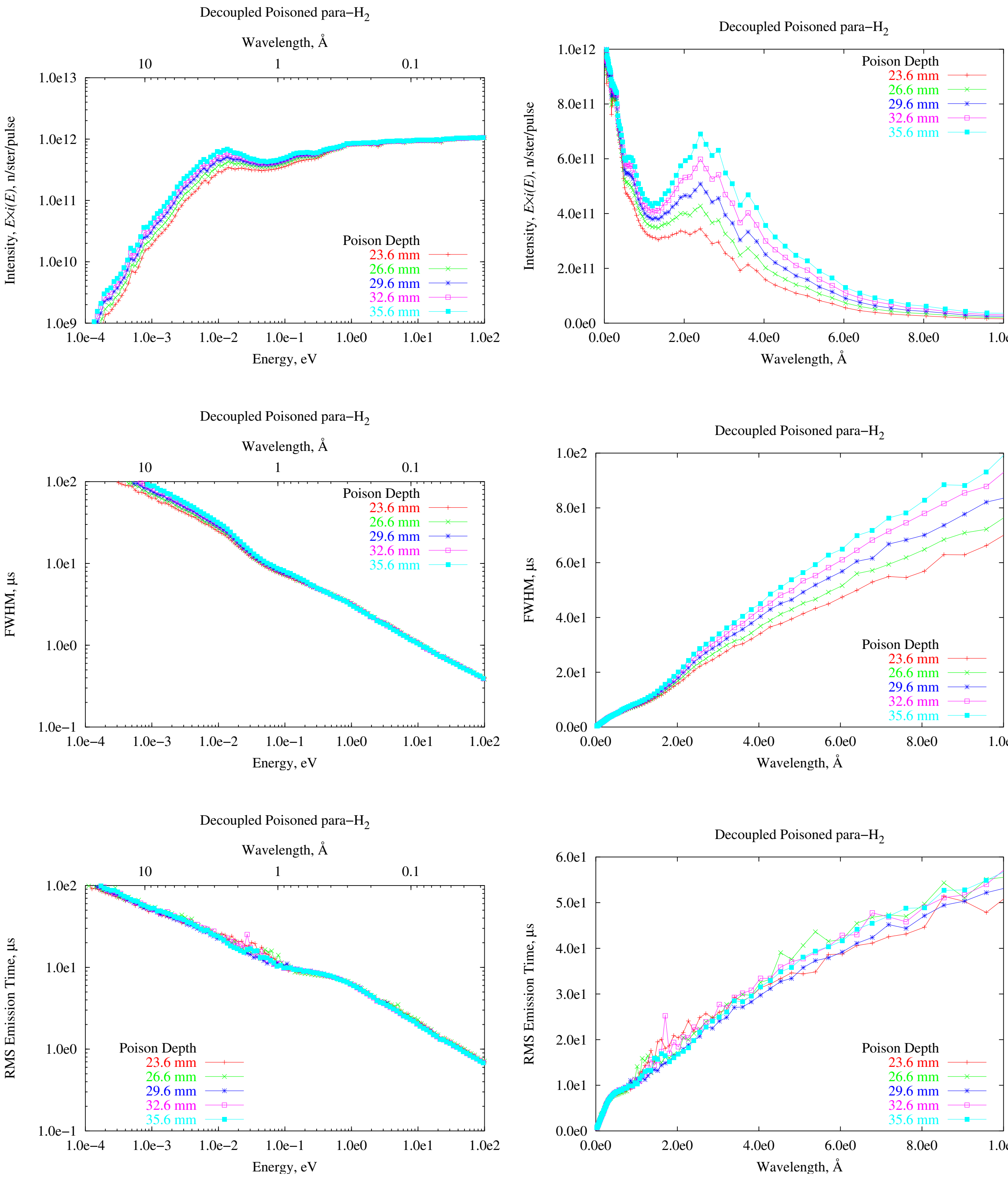

Figure 7: Intensity and pulse widths (FWHM and RMS) for decoupled parahydrogen moderators with different poison depths.

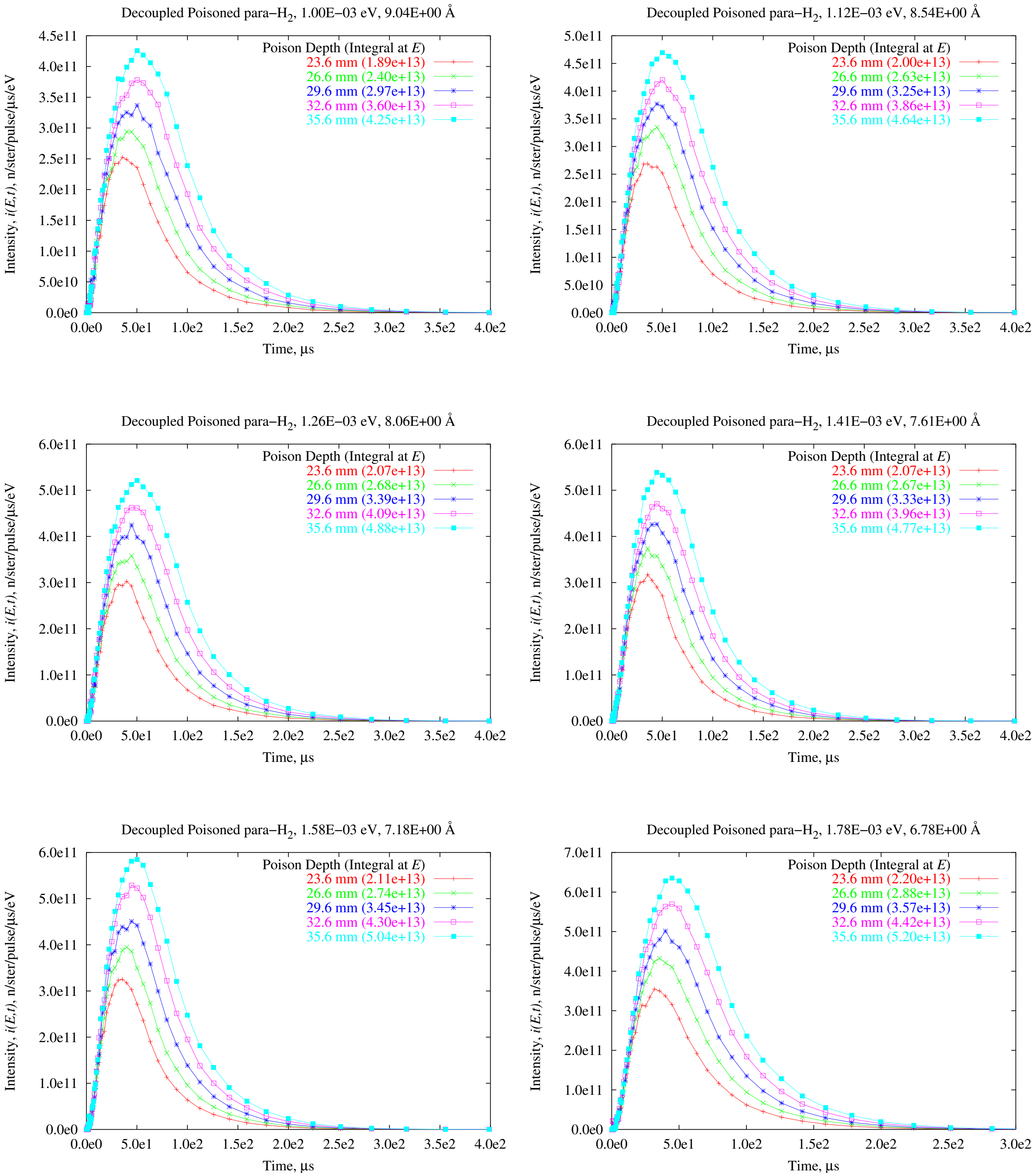

Figure 8: Emission time distributions for decoupled parahydrogen moderators with different poison depths.

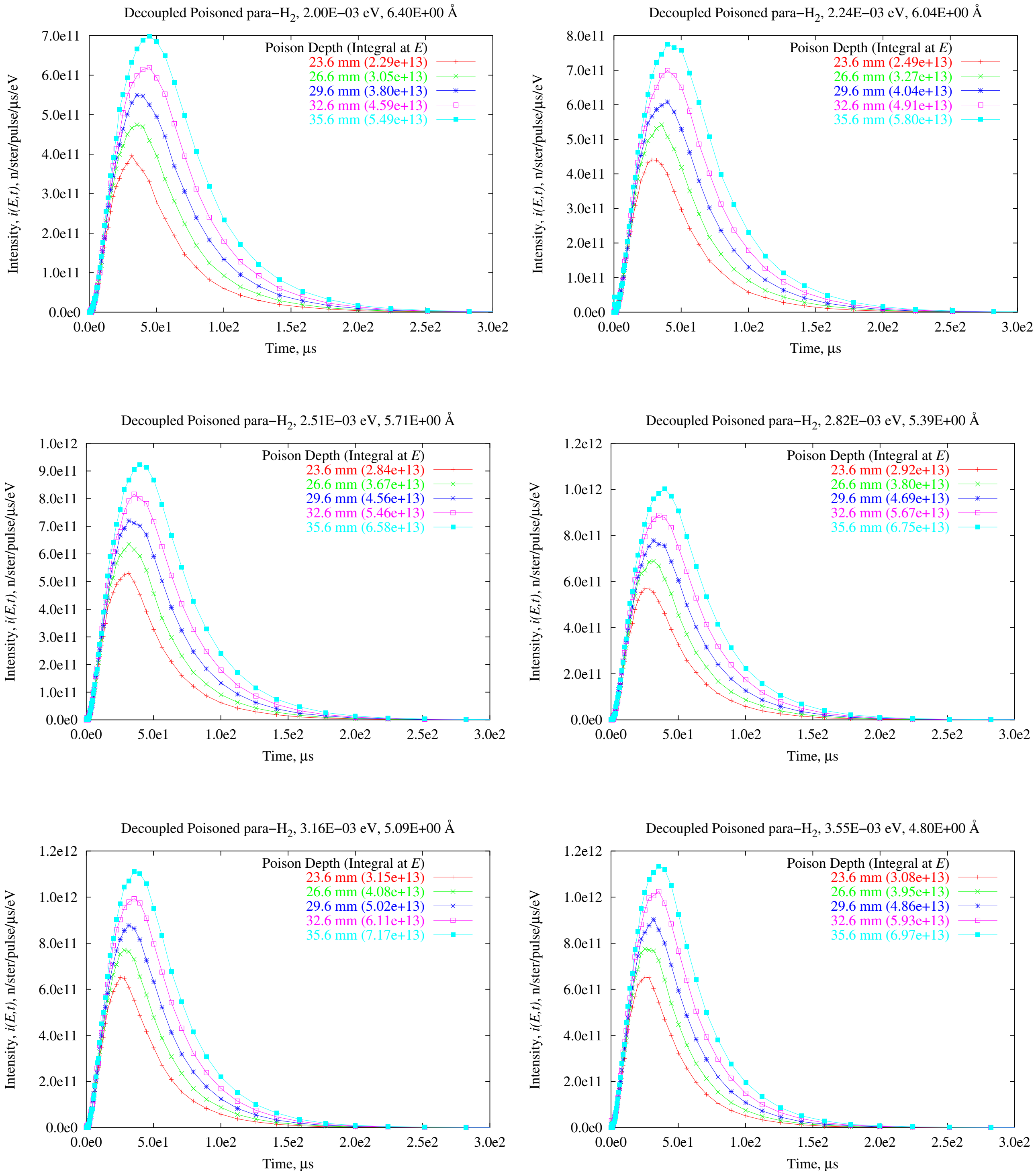

Figure 9: Emission time distributions for decoupled parahydrogen moderators with different poison depths.

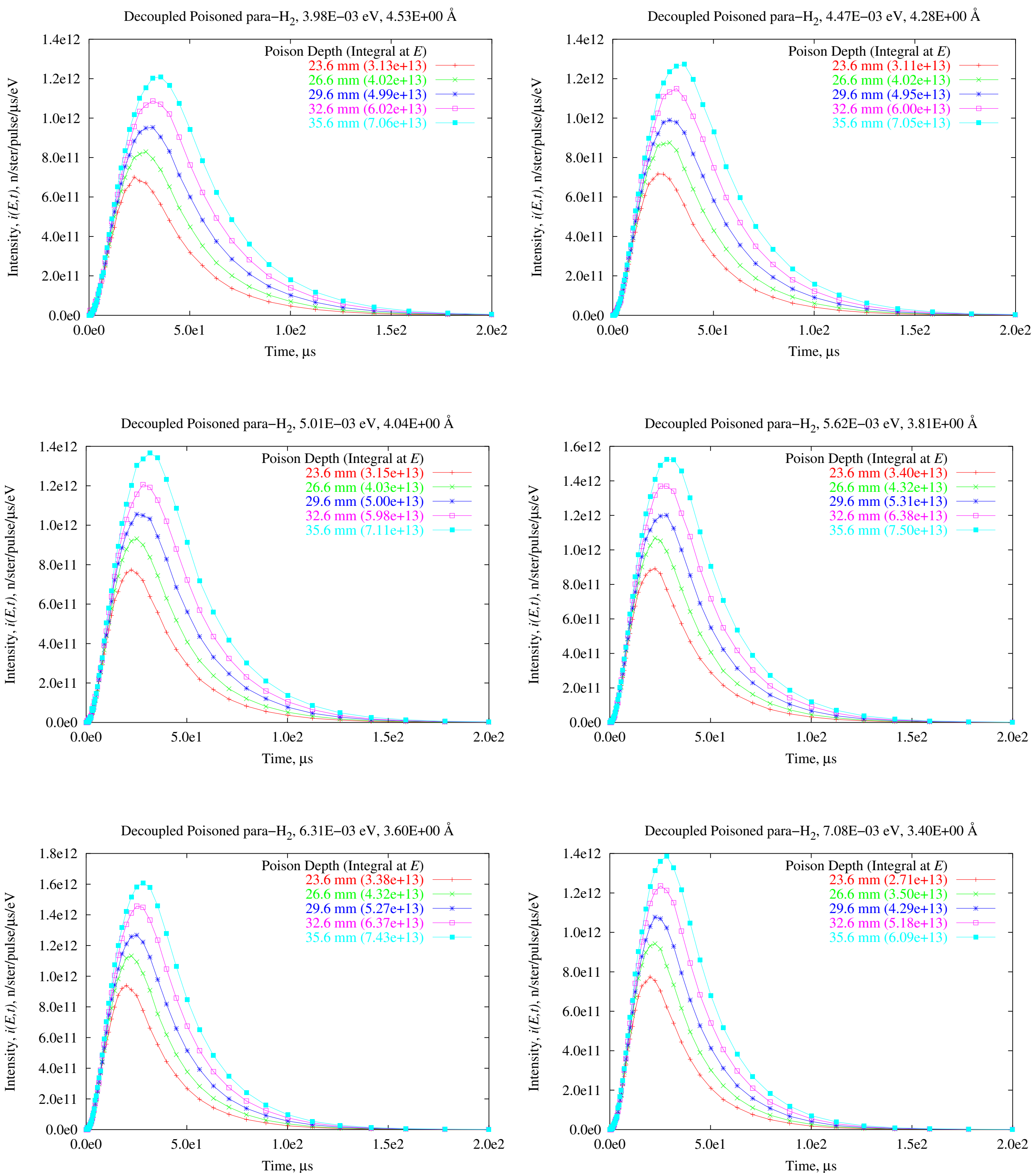

Figure 10: Emission time distributions for decoupled parahydrogen moderators with different poison depths.

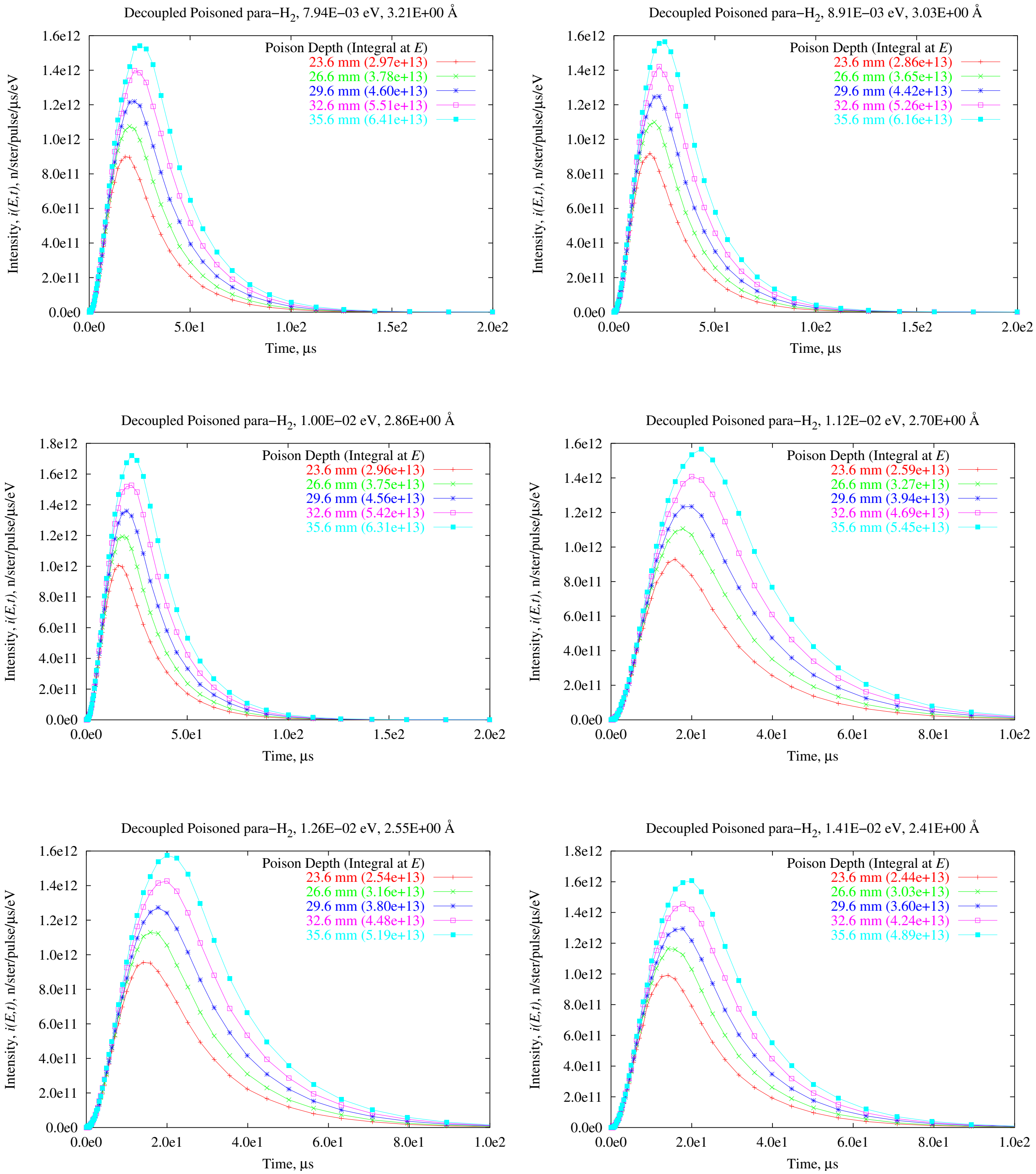

Figure 11: Emission time distributions for decoupled parahydrogen moderators with different poison depths.

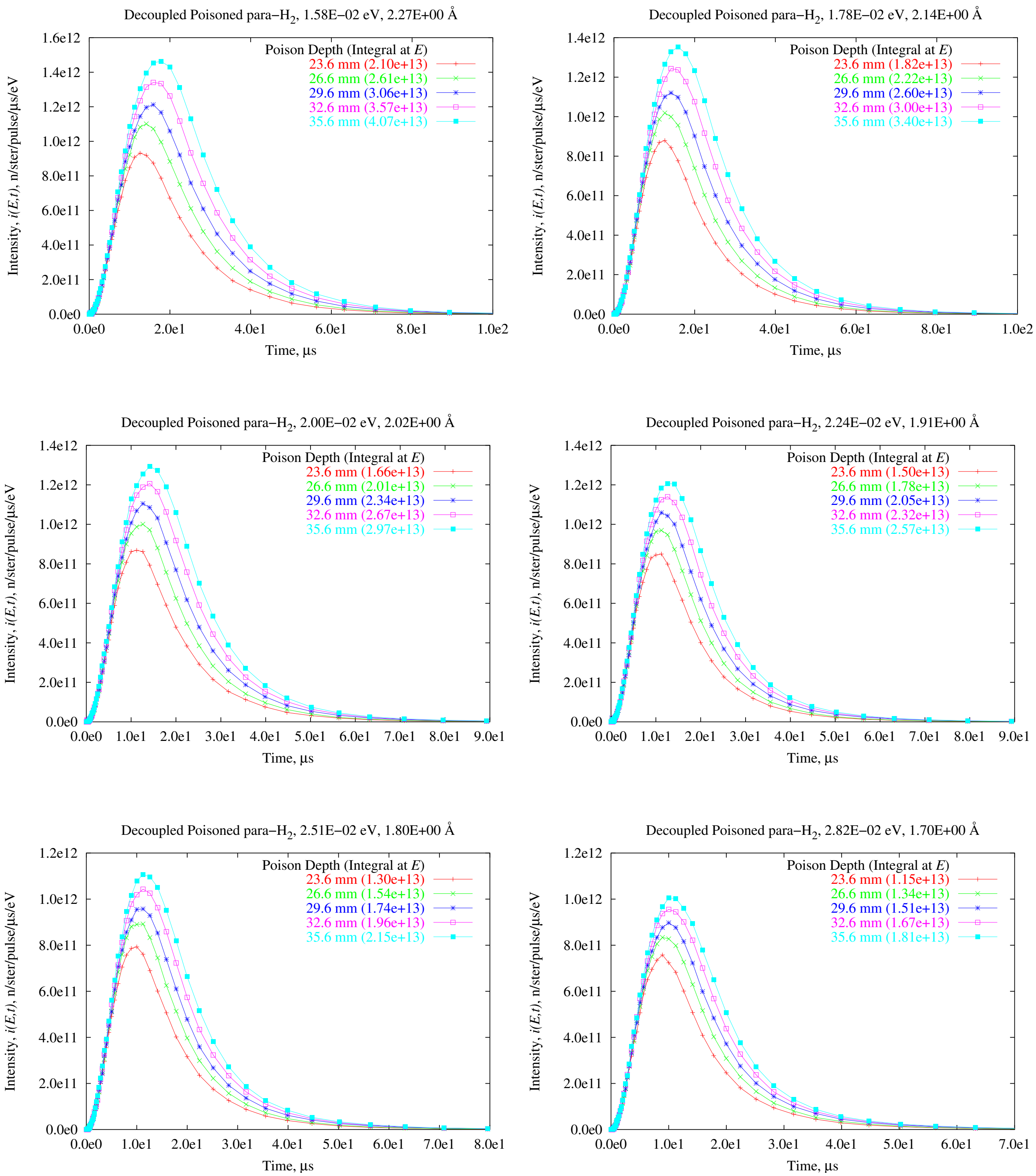

Figure 12: Emission time distributions for decoupled parahydrogen moderators with different poison depths.

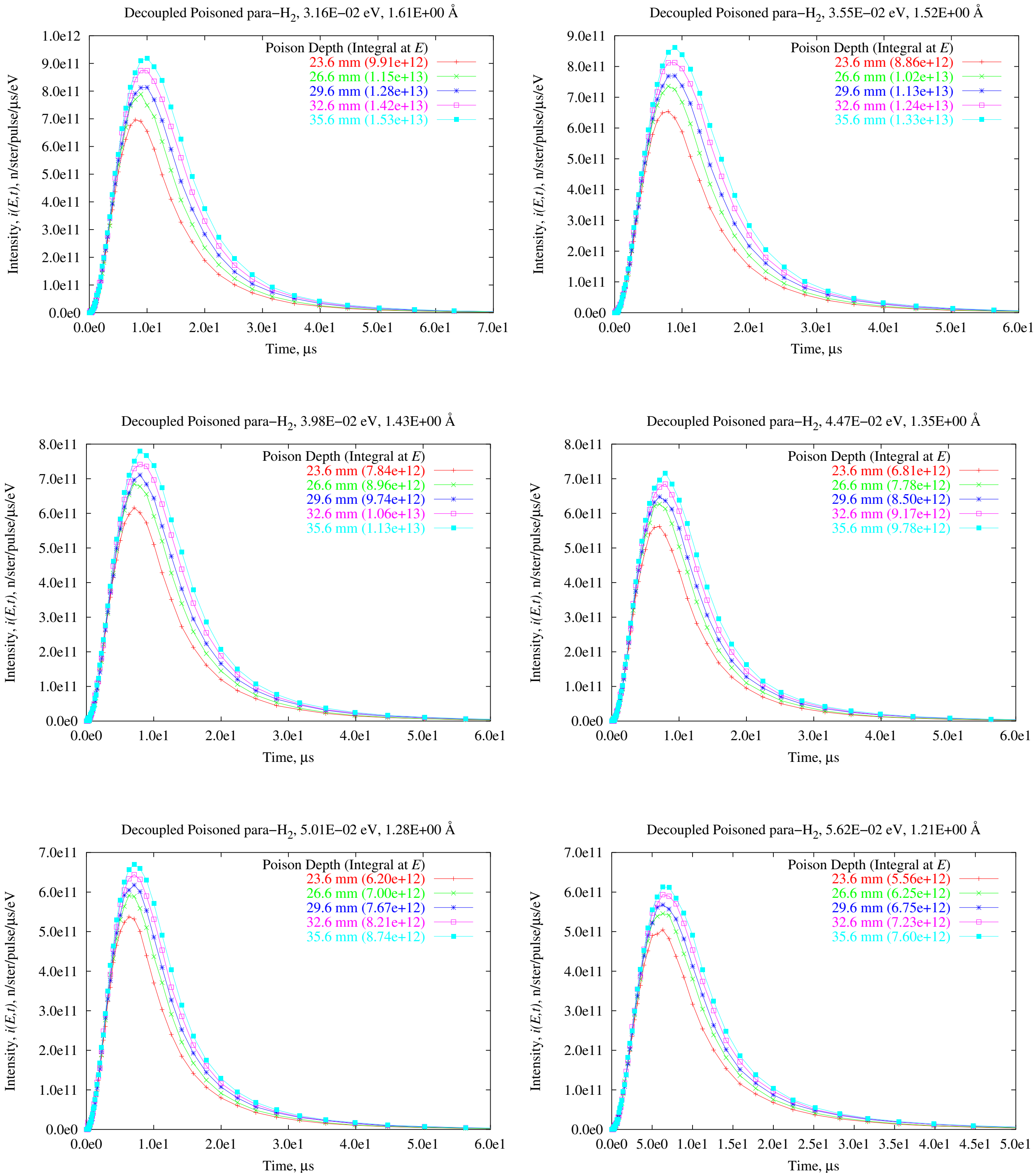

Figure 13: Emission time distributions for decoupled parahydrogen moderators with different poison depths.

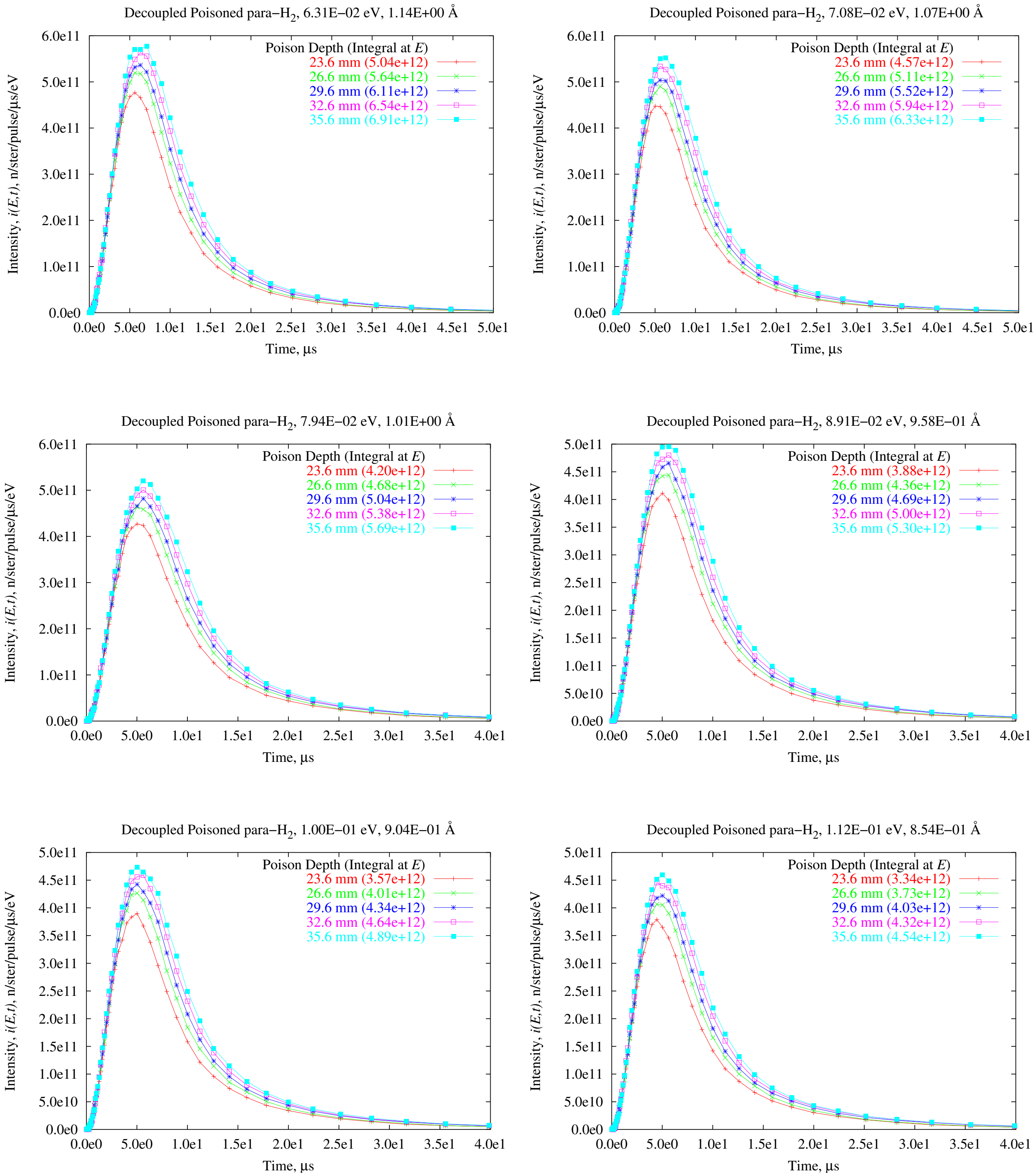

Figure 14: Emission time distributions for decoupled parahydrogen moderators with different poison depths.

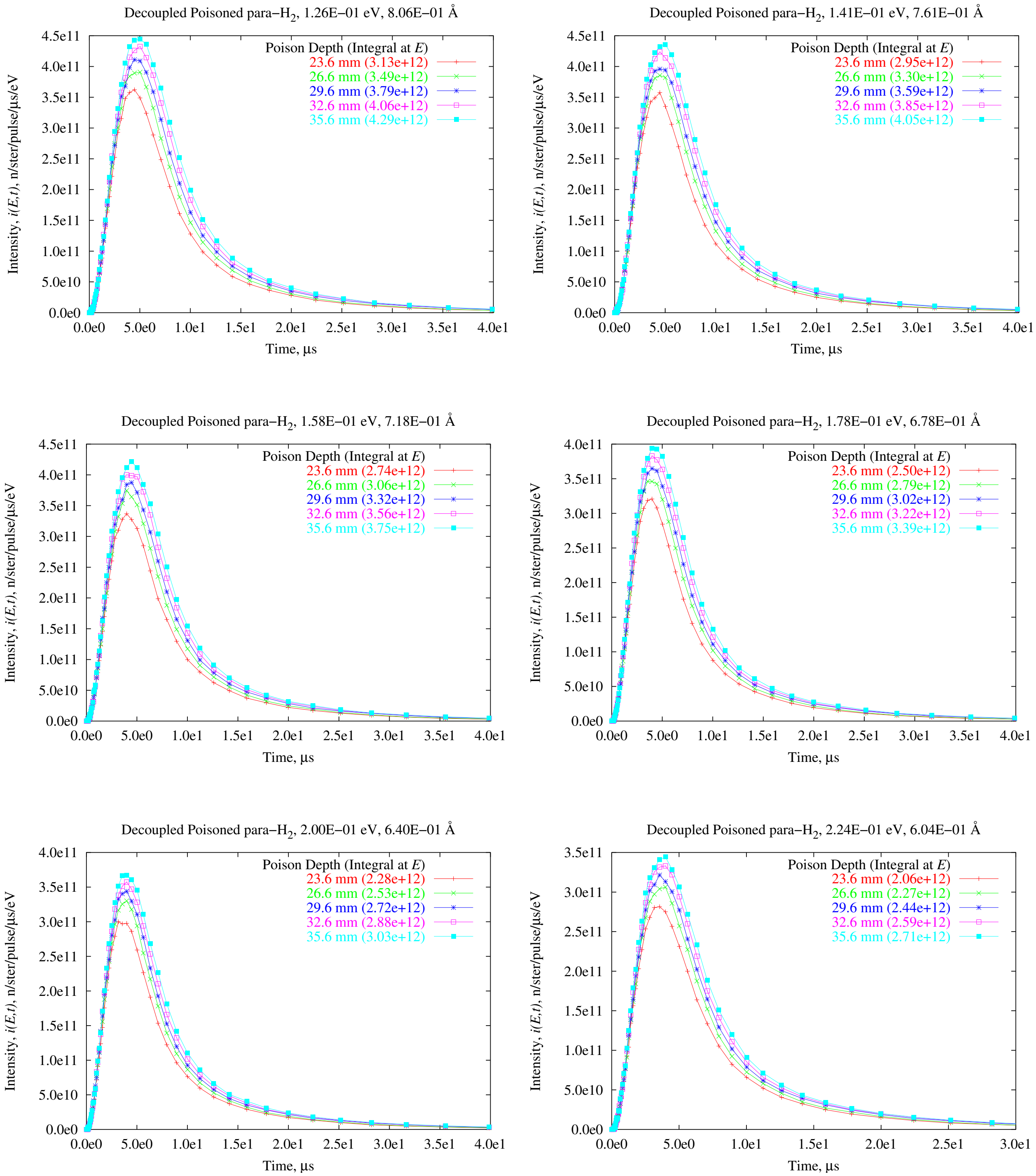

Figure 15: Emission time distributions for decoupled parahydrogen moderators with different poison depths.

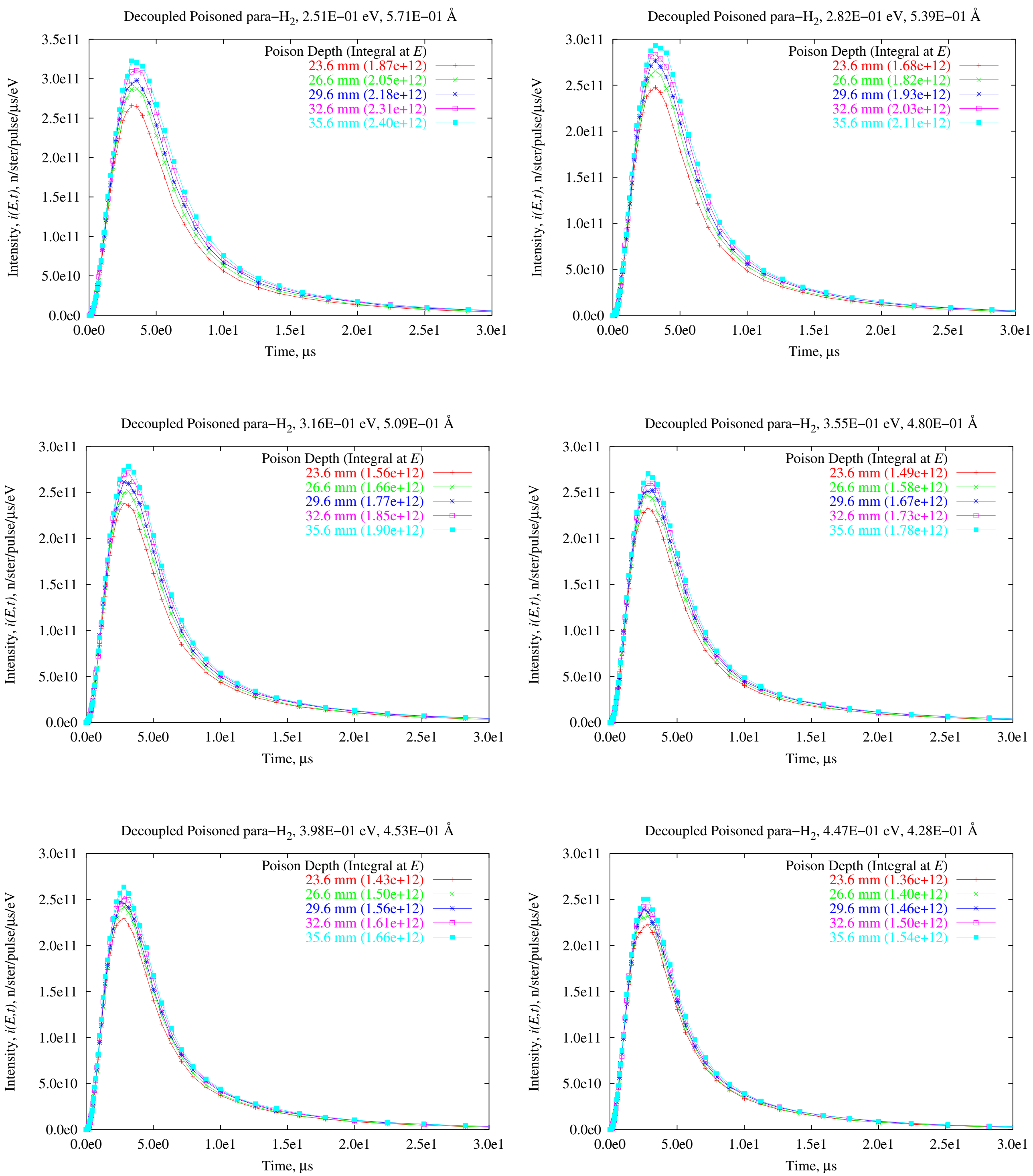

Figure 16: Emission time distributions for decoupled parahydrogen moderators with different poison depths.

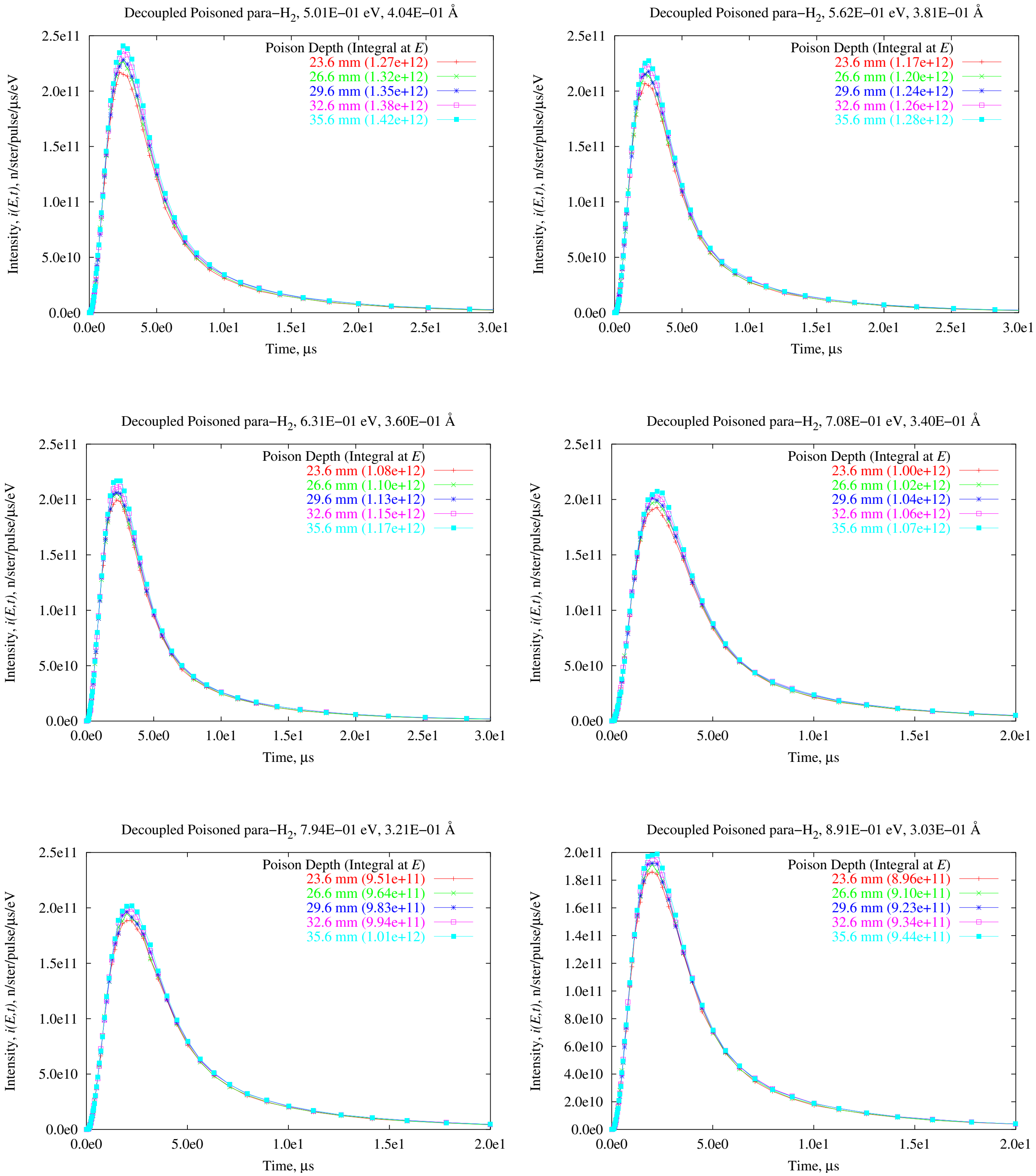

Figure 17: Emission time distributions for decoupled parahydrogen moderators with different poison depths.

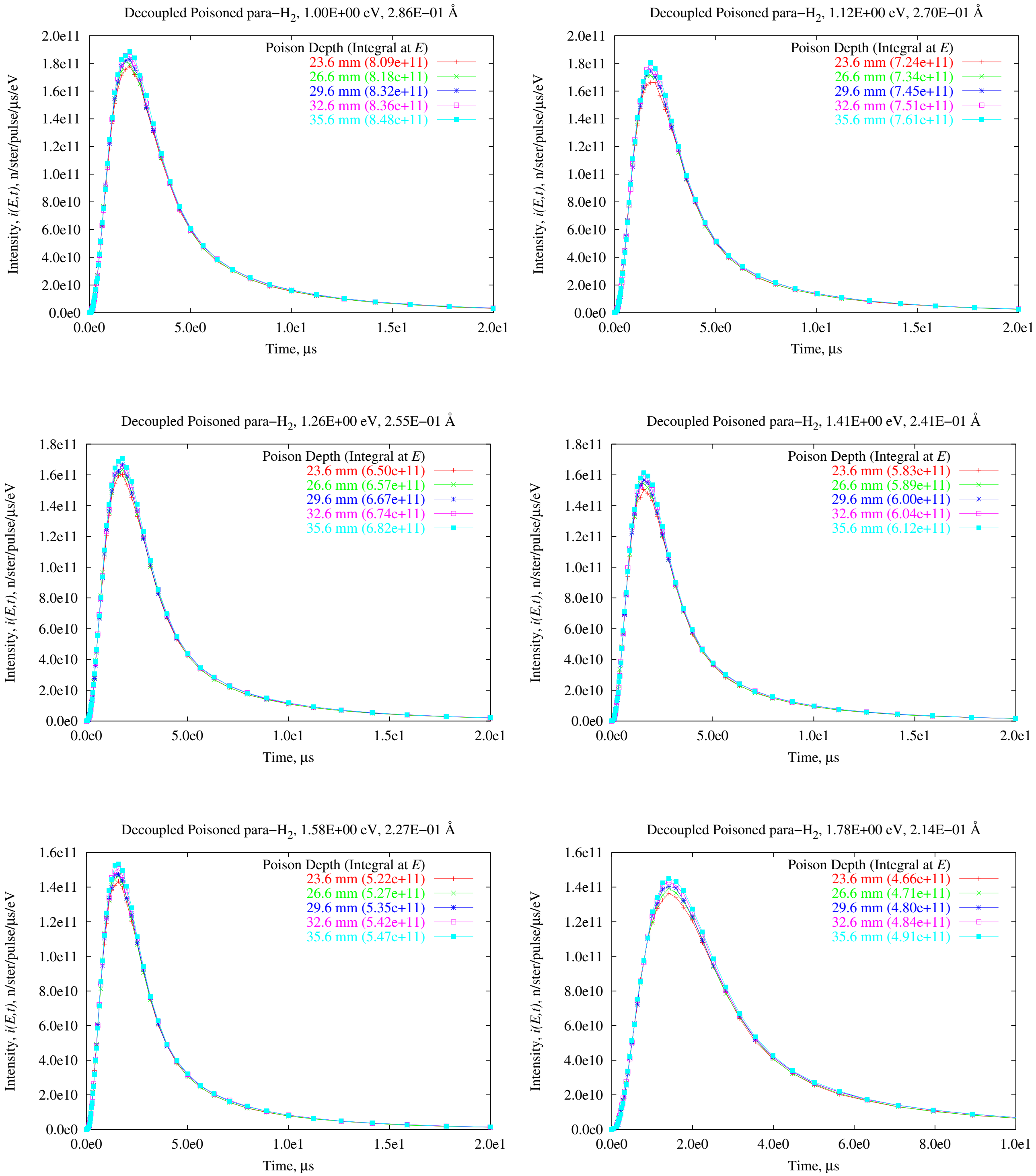

Figure 18: Emission time distributions for decoupled parahydrogen moderators with different poison depths.

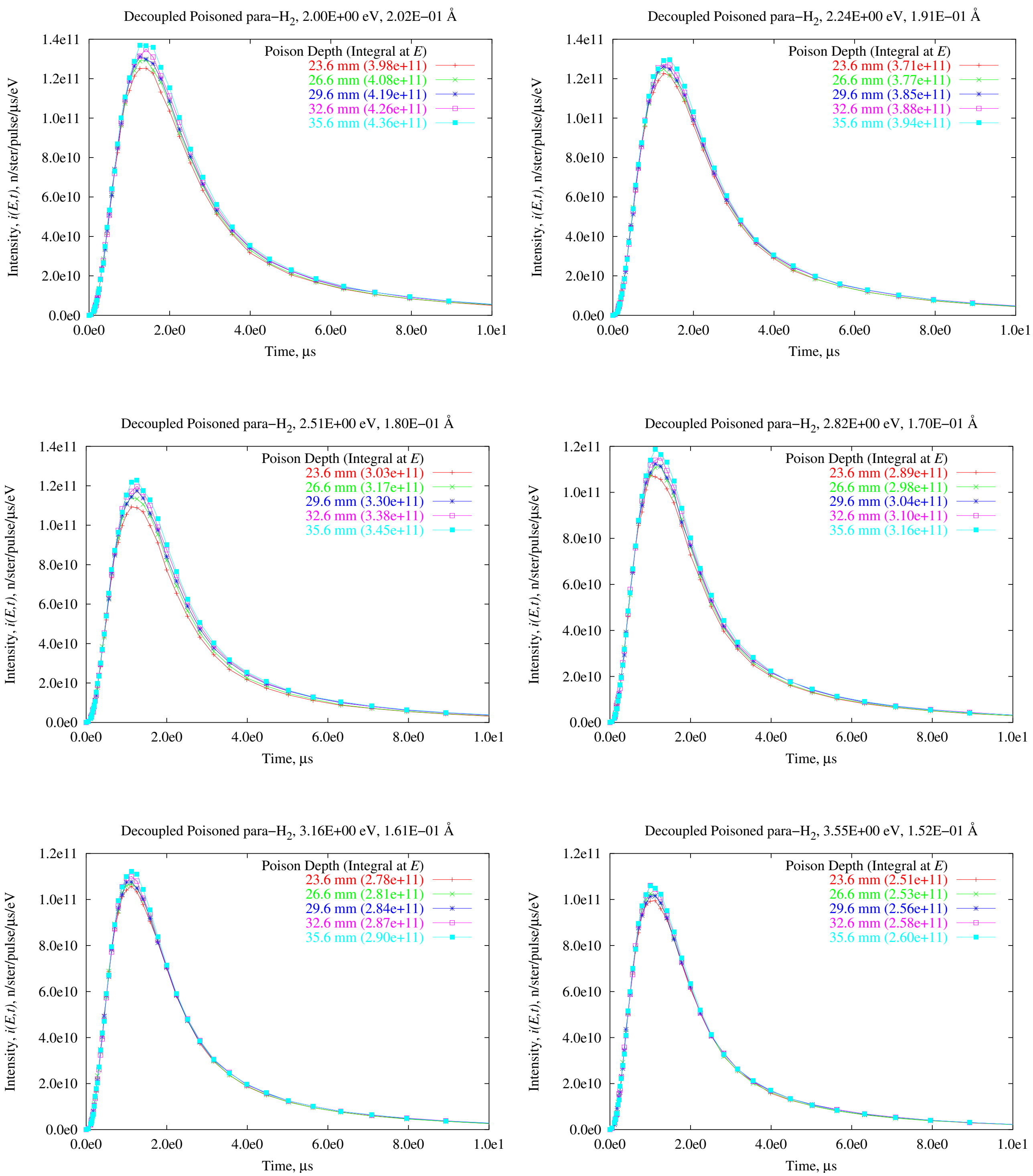

Figure 19: Emission time distributions for decoupled parahydrogen moderators with different poison depths.

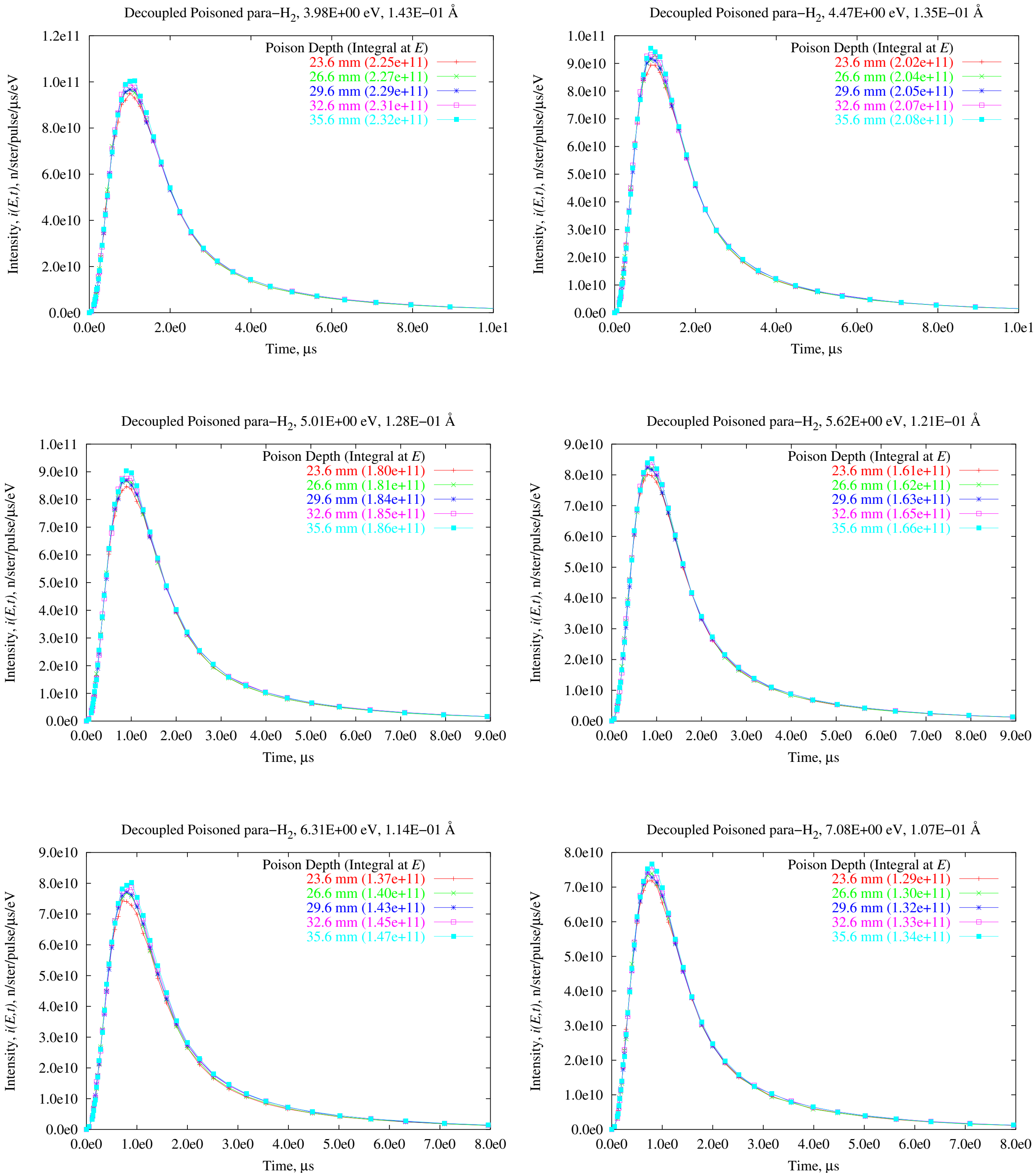

Figure 20: Emission time distributions for decoupled parahydrogen moderators with different poison depths.

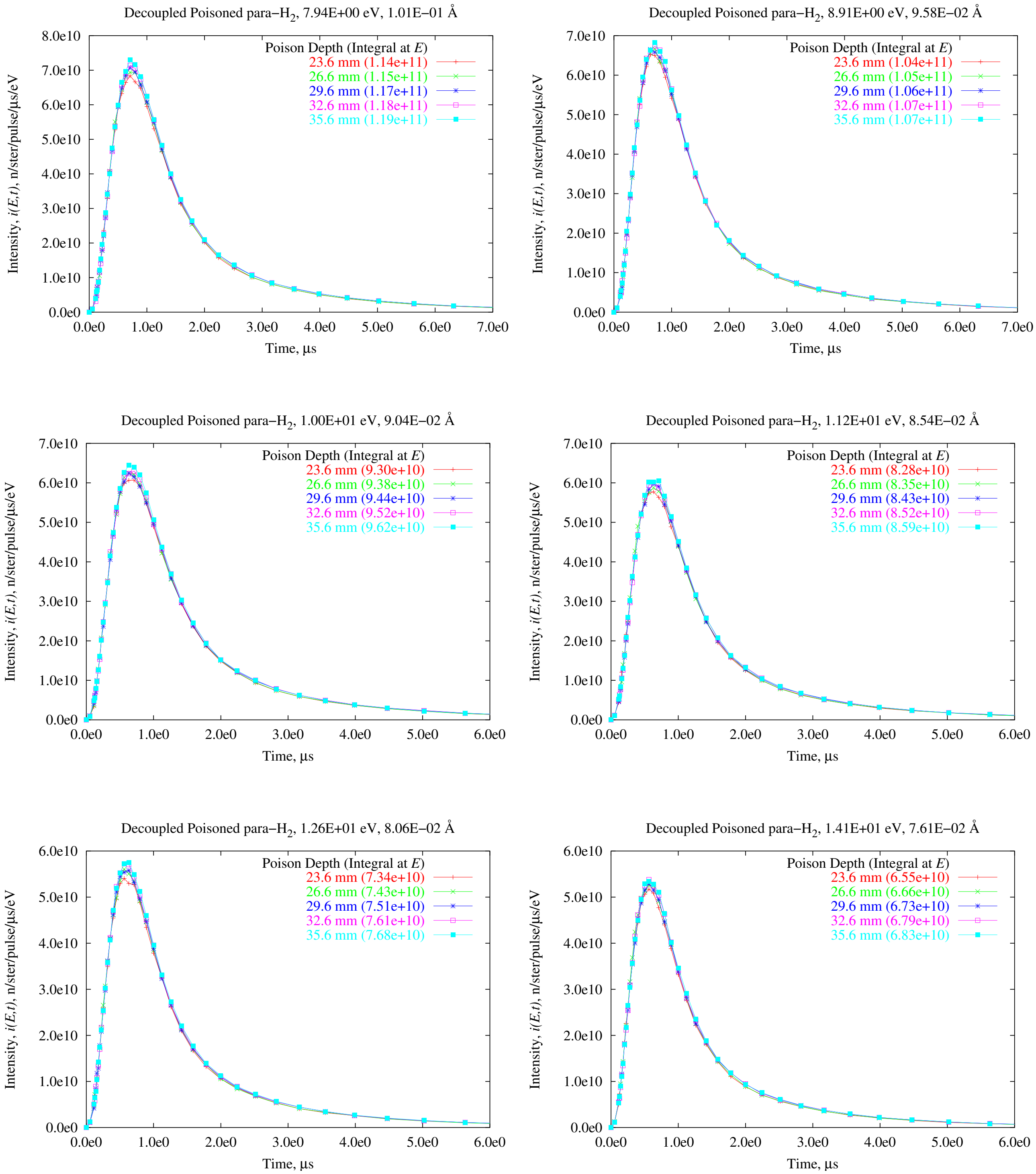

Figure 21: Emission time distributions for decoupled parahydrogen moderators with different poison depths.